Published in final edited form as:
J Comput Neurosci. 2013 August ; 35(1): 1–17. doi:10.1007/s10827-012-0436-2.

Biophysical mechanism of spike threshold dependence on the rate of rise of the membrane potential by sodium channel inactivation or subthreshold axonal potassium current

Jason C. Wester and
Department of Neuroscience, University of Pennsylvania Perelman School of Medicine, Philadelphia, PA 19104, USA

Diego Contreras
Department of Neuroscience, University of Pennsylvania Perelman School of Medicine, Philadelphia, PA 19104, USA; Department of Neuroscience, University of Pennsylvania Perelman School of Medicine, 215 Stemmler Hall, Philadelphia, PA 19106-6074, USA

Abstract

Spike threshold filters incoming inputs and thus gates activity flow through neuronal networks. Threshold is variable, and in many types of neurons there is a relationship between the threshold voltage and the rate of rise of the membrane potential (dVm/dt) leading to the spike. In primary sensory cortex this relationship enhances the sensitivity of neurons to a particular stimulus feature. While Na^+ channel inactivation may contribute to this relationship, recent evidence indicates that K^+ currents located in the spike initiation zone are crucial. Here we used a simple Hodgkin-Huxley biophysical model to systematically investigate the role of K^+ and Na^+ current parameters (activation voltages and kinetics) in regulating spike threshold as a function of dVm/dt. Threshold was determined empirically and not estimated from the shape of the Vm prior to a spike. This allowed us to investigate intrinsic currents and values of gating variables at the precise voltage threshold. We found that Na^+ inactivation is sufficient to produce the relationship provided it occurs at hyperpolarized voltages combined with slow kinetics. Alternatively, hyperpolarization of the K^+ current activation voltage, even in the absence of Na^+ inactivation, is also sufficient to produce the relationship. This hyperpolarized shift of K^+ activation allows an outward current prior to spike initiation to antagonize the Na^+ inward current such that it becomes self-sustaining at a more depolarized voltage. Our simulations demonstrate parameter constraints on Na^+ inactivation and the biophysical mechanism by which an outward current regulates spike threshold as a function of dVm/dt.

Keywords

Spike threshold; Hodgkin-Huxley model; Potassium current; Sodium channel inactivation; dVm/dt

1 Introduction

The voltage threshold for spike initiation is a critically important non-linearity in the process by which presynaptic inputs are integrated by a neuron. Spike threshold allows cells to filter incoming inputs and effectively contributes to response selectivity. Importantly, spike threshold is variable, which permits adjustment of neuronal sensitivity and may play a role

Correspondence to: Diego Contreras.

in gating information flow through a neuron. In particular, spike threshold is dependent on the rate of rise of the membrane potential (dVm/dt) leading to the spike. Thus, faster dVm/dt is associated with a more hyperpolarized spike threshold, whereas slower dVm/dt is associated with a more depolarized threshold. This relationship has been observed in a variety of brain regions from numerous species, including the axon of the squid (Hodgkin and Huxley 1952; Noble and Stein 1966), neurons of brainstem auditory nuclei (Ferragamo and Oertel 2002), spinal motor neurons (Schlue et al. 1974), neurons of Aplysia (Bryant and Segundo 1976), and cortical neurons of the hippocampus, motor cortex, and sensory cortex (Azouz and Gray 2000; Henze and Buzsaki 2001; Azouz and Gray 2003; Wilent and Contreras 2005; Higgs and Spain 2011). In rat primary somatosensory cortex, this relationship results in neurons being more sensitive to whisker deflection in the preferred direction (Wilent and Contreras 2005). In mouse ventral cochlear nucleus, this relationship results in spike failure for inputs that fail to drive the membrane potential (Vm) at a rate of at least 5 mV/ms (Ferragamo and Oertel 2002). In both cases, the net effect is that these neurons have an intrinsic sensitivity to strong synchronous inputs. Similar results were found in cat primary visual cortex (Azouz and Gray 2000, 2003; Cardin et al. 2010).

A possible simple mechanism for the relationship between dVm/dt and spike threshold is the accumulation of Na^+ channel inactivation when the Vm rises slowly, as originally described for spike initiation in the squid giant axon (Hodgkin and Huxley 1952; Noble 1966; Noble and Stein 1966). Indeed, this was assumed to be the primary mechanism in many studies showing this relationship (Azouz and Gray 2000; Henze and Buzsaki 2001; Azouz and Gray 2003; Wilent and Contreras 2005). However, there are potassium currents located in the axon that activate at sub-threshold voltages (Rudy 1988), and thus can influence spike initiation. In particular, a current mediated by Kv1 channels, also called the D-current (originally described by Storm (1988)), activates at sub-threshold voltages, has fast activation kinetics, very slow inactivation kinetics, and plays a prominent role in regulating neuronal excitability and spike threshold (Bekkers and Delaney 2001). Block of the D-current results in a hyperpolarized threshold, a faster rising Vm prior to spiking, and increased spike frequency (Storm 1988; Bekkers and Delaney 2001; Dodson et al. 2002; Guan et al. 2007; Goldberg et al. 2008). Indeed, this current is directly responsible for the sensitivity of auditory brainstem neurons to very fast dVm/dt values described above (Ferragamo and Oertel 2002). Furthermore, the D-current was recently found to mediate the relationship between dVm/dt and spike threshold in layer 2/3 pyramidal neurons in rat motor cortex (Higgs and Spain 2011).

Here we explore the biophysical mechanism by which intrinsic membrane currents in the axon influence the relationship between dVm/dt and spike threshold. We use a simple biophysical model to explore the interaction of Na^+ and K^+ currents at action potential threshold, which was determined empirically rather than estimated from the Vm trajectory. Thus we could precisely define the intrinsic membrane currents and the instantaneous values of their gating variables at the true threshold. We used models of a single cortical Na^+ (inward) current and single K^+ (outward) current as described by Traub and Miles (1991) and Mainen et al. (1995) for cortical pyramidal neurons. We systematically adjusted the activation voltages and kinetics of each current in order to precisely understand the roles of Na^+ inactivation and K^+ currents in producing the relationship. Na^+ inactivation alone could produce a relationship, but only when inactivation was sufficiently hyperpolarized and inactivation kinetics were slow. Furthermore, we found that hyperpolarization of the voltage activation of the K^+ current alone was sufficient to observe the relationship. This resulted in an outward current at sub-threshold voltages that antagonized the Na^+ current in order to prevent it from becoming self-sustained at a fixed voltage threshold. Na^+ channel inactivation was not necessary to mediate the relationship when this outward current was

present. Thus our simulations provide a biophysical mechanism by which a sub-threshold K^+ current regulates spike threshold.

2 Methods

2.1 Hodgkin-Huxley model for Na^+ and K^+ currents

We used the Hodgkin and Huxley (1952) model of voltage-gated membrane currents responsible for the generation of an action potential:

$$I_{Na} = \overline{g}_{Na} m^3 h (V - E_{Na}),$$
$$I_K = \overline{g} K^{n^4} (V - E_K).$$

In these equations, $\overline{g}_{Na}$ and $\overline{g}_K$ are the maximum conductance values for Na^+ and K^+ respectively. The variables m, h, and n represent gating variables for the channels; m and h represent activation and inactivation gates for Na^+, and n represents an activation gate for K^+. In this study we manipulated these variables in order to understand the interactions of Na^+ and K^+ currents during spike initiation. In the Hodgkin-Huxley model, Na^+ current requires three independent activation gates (thus the term m^3) and one inactivation gate, and K^+ current requires four independent activation gates (thus n^4). The term m^3h represents the fraction of Na^+ channels available, and n^4 the fraction of K^+ channels available. These variables obey the equations:

$$\frac{dm}{dt} = \frac{-1}{\tau_m(V)} (m - m_\infty (V)),$$
$$\frac{dh}{dt} = \frac{-1}{\tau_h(V)} (h - h_\infty (V)),$$
$$\frac{dn}{dt} = \frac{-1}{\tau_n(V)} (n - n_\infty (V)),$$

where

$$m_\infty (V) = \frac{\alpha(V)}{\alpha(V)+\beta(V),}$$
$$\tau_m (V) = \frac{1}{\alpha(V)+\beta(V)},$$

and h_∞ and n_∞ (and thus τ_h and τ_n) follow the same equations. The variable m_∞ represents the steady-state activation of Na^+ current, and is a value between 0 and 1 as a function of membrane voltage. τ_m is the time constant of the current and determines how quickly steady-state values are reached. α and β are the forward and backward rate constants for the gating variables as described below.

2.2 Channel models used in this study

We used three different sets of rate constants for cortical pyramidal neurons at 36 ° C: 1) Traub and Miles (1991) (referred to as “Traub (default)”), 2) Mainen et al. (1995) (referred to as “Mainen”), and 3) a hybrid of these two models (referred to as “Traub (adjusted)”).

1) TRAUB (DEFAULT):

$$\alpha_m = -0.32\,(V - V_{\mathrm{SHIFT}} - 13) / (\exp[-(V - V_{\mathrm{SHIFT}} - 13)/4] - 1),$$
$$\beta_m = 0.28\,(V - V_{\mathrm{SHIFT}} - 40) / (\exp[(V - V_{\mathrm{SHIFT}} - 40)/5] - 1),$$
$$\alpha_h = 0.128\exp[-(V - V_{\mathrm{SHIFT}} - 17)/18],$$
$$\beta_h = 4/(1+\exp[-(V - V_{\mathrm{SHIFT}} - 40)/5]),$$
$$\alpha_n = (-0.032\,(V - V_{\mathrm{SHIFT}} - 15)) / (\exp(-(V - V_{\mathrm{SHIFT}} - 15)/5) - 1),$$
$$\beta_n = 0.5\exp[-(V - V_{\mathrm{SHIFT}} - 10)/40].$$

In these equations, V is the membrane potential. An important variable for the purpose of this study is V_{SHIFT}, a constant that shifts the half-activation voltage of m, h, and n, and their associated time constants (in units of mV). V_{SHIFT} is equivalent to the variable V_T as described in Destexhe and Sejnowski (2001), renamed here for clarity. Throughout this study, these variables were used to adjust the voltage-dependence of K^+ activation and Na^+ inactivation in the axon (hillock and initial segment compartments). $V_{SHIFT(m)}$ denotes the value of V_{SHIFT} applied to both α_m and β_m, $V_{SHIFT(m,h)}$ denotes the value of V_{SHIFT} applied to α_m, β_m, α_h, and β_h, etc. The steady-state activation curves and their time constants for Na^+ and K^+ according to the rate constants defined above (with $V_{SHIFT(m,h,n)} = -63$) are shown in Fig. 1.

2) MAINEN:

$$\alpha_m = 0.182\,(-35 - V) / (\exp[(-35 - V)/9] - 1),$$
$$\beta_m = 0.124\,(V - -35) / (\exp[(V - -35)/9] - 1),$$
$$\alpha_h = 0.024\,(-50 - V) / \exp[(-50 - V)/5] - 1),$$
$$\beta_h = 0.0091\,(V - -75) / (\exp[(V - -75)/5] - 1),$$
$$\alpha_n = (0.02\,(-(V - 25)) / \exp[-(V - 25)/9] - 1),$$
$$\beta_n = (0.002\,(V - 25) / (\exp[(V - 25)/9] - 1).$$

3) TRAUB (ADJUSTED):

$$\alpha_h = 0.128\exp[-(V - V_{\mathrm{SHIFT}} - 17)/30],$$
$$\beta_h = 4/(1+\exp(-(V - V_{\mathrm{SHIFT}} - 40)/7.2)),$$
$$V_{\mathrm{SHIFT}(h)} = -81$$

The rate constants α_m, β_m, α_n, and β_n are as described for Traub (default) above, and $V_{SHIFT(m,n)} = -63$. The adjustment to α_h and β_h results in an h_∞ curve that matches that from Mainen (see Fig. 8(a)).

2.3 Multi-compartment model properties

All computational models were run using the NEURON simulation environment (Hines and Carnevale 1997). Unless otherwise specified, simulations were performed using a three-compartment model consisting of a soma and axon (with hillock and initial segment compartments) (See Fig. 2). All compartments followed the membrane equation:

$$C_m \frac{dV}{dt} = -g_L\,(V - EL) - I_{Na} - I_K,$$

Where is C_m the membrane capacitance (1 μF/cm^2), g_L is the leak conductance (0.097 mS/cm^2), E_L is the leak reversal potential (−70 mV), and I_{Na} and I_K are the currents defined

above. Parameters for passive properties were taken from a model of a layer 5 cortical pyramidal neuron (Contreras et al. 1997), with the exception of E_L which was chosen for a resting potential of −70 mV. For each compartment, axial resistance was 384Ω/cm, E_{Na} was 50 mV, and E_K was −90 mV.

Soma compartment—The soma was modeled as a cylinder with a length of 43 μm and diameter of 23 μm, based on the dimensions of a reconstructed layer 5 pyramidal neuron (Contreras et al. 1997). For Traub (default) and Traub (adjusted) models, the conductance density for Na^+ was 70 ps/μm^2 and the density for K^+ was 200 ps/μm^2 as described in Contreras et al. (1997). For the Mainen model, the conductance density for Na^+ was 750 ps/μm^2 and the density for K^+ was 320 ps/μm^2, similar to Yu et al. (2008).

Axon—The axon consisted of two cylindrical compartments: a hillock with length 5 μm and diameter 4 μm, and an initial segment with length 15 μm and diameter 1 μm. For Traub (default) and Traub (adjusted) models, the conductance density for Na^+ was 30,000 ps/μm^2 and the density for K^+ was 2,000 ps/μm^2 as described in Contreras et al. (1997). For the Mainen model, the conductance density for Na^+ was 7,500 ps/μm^2 and the density for K^+ was 1,600 ps/μm^2, similar to Yu et al. (2008). Conductance densities were the same in both the hillock and initial segment compartments.

2.4 Single compartment model properties

A single compartment similar to that described in Destexhe et al. (2001) was also used. Length and diameter were both 105 μm. C_m=1 μF/cm^2, g_L=0.045 mS/cm^2, E_L=−70 mV. Axial resistance was 250Ω/cm. E_{Na} was 50 mV, and E_K was −90 mV. I_{Na} and I_K were as described above for Traub (default) with conductance densities of 516 ps/μm^2 for Na^+ and for 100 ps/μm^2 for K^+.

2.5 Analysis

All simulations generated in NEURON were imported to Igor (Wavemetrics) and analyzed with custom routines.

3 Results

Our goal was to use a simple biophysical model to understand the interactions between inward and outward currents that result in the relationship between dVm/dt and spike threshold observed experimentally in a variety of neurons both *in vivo* and *in vitro*. We used Hodgkin-Huxley models of cortical Na^+ and K^+ currents and systematically adjusted the voltage dependence of the currents as well as their kinetics (see Section 2). Our simulation design allowed for a detailed analysis of the intrinsic currents and the values of their gating variables at the true voltage threshold in order to determine the biophysical mechanism that produces the relationship.

3.1 Computational model and simulation design

We used a three compartment biophysical model consisting of a soma, axon hillock, and axon initial segment (Fig. 2(a)) (see Section 2 for details). For simplicity we used only two voltage-gated currents (one Na^+ and one K^+) modeled using the Hodgkin-Huxley formalism (Hodgkin and Huxley 1952) as described by Traub and Miles (1991) or Mainen et al. (1995) for cortical pyramidal neurons (see Section 2). Importantly, we used a single potassium current in the form of the delayed-rectifier for which parameters have been extensively studied and modeled. Our goal was to understand how the general properties of net inward and outward currents result in a relationship between dVm/dt and spike threshold. For that

reason we chose to start our investigation with a simple and well known set of voltage activation and kinetic parameters which could be systematically adjusted.

In order to control the dVm/dt leading to spike initiation, we injected ramps of current with different slopes at the soma. In all cases, action potentials were initiated in the axon initial segment and back-propagated to the soma compartment (Fig. 2(b)) as described for cortical pyramidal neurons (Mainen et al. 1995; Stuart et al. 1997; Palmer and Stuart 2006; Shu et al. 2007b). We developed a novel approach to precisely define spike threshold, rather than rely on estimates such as the maximum of the second derivative of the Vm prior to the spike or phase plane analysis of dVm/dt as a function of Vm (Wilent and Contreras 2005; Yu et al. 2008). Our method allowed us to measure and compare spike thresholds across compartments and simulation conditions with a high precision (within 0.1 mV of true spike threshold). We determined the voltage threshold for spike initiation empirically by stepwise increasing the duration of the current ramps, such that each step led to an additional 0.1 mV depolarization in the soma compartment until a spike was triggered in the axon (Fig. 2(c)). We defined spike threshold as the Vm at the time of ramp offset, after which point Na^+ current alone drove the Vm response (Fig. 2(c), bottom right). Thus, 0.1 mV hyperpolarized to this Vm was subthreshold and resulted in spike failure, while 0.1 mV depolarized to this Vm was suprathreshold for spike initiation (Fig. 2(c)). In this manner, spike initiation was due purely to activation of sufficient axonal Na^+ current, and was not contaminated by additional stimulus current. Furthermore, our method allowed us to precisely measure ionic currents and gating variables for Na^+ and K^+ channels at true spike threshold.

Even though the ramps were always injected in the soma, we defined the spike threshold separately in the soma and axon initial segment compartments at the time of ramp offset. We emphasize that the true spike threshold is the Vm value recorded in the axonal compartment at the time of ramp offset, as spikes recorded in the soma are back-propagating action potentials. Thus we focus our analysis on the axon initial segment compartment, however we also report action potential thresholds in the soma as this is the site of recording in most experiments with real neurons due to accessibility.

3.2 The Traub (default) model produces a fixed spike threshold unless the voltage dependence of Na^+ inactivation is shifted by 20 mV

We started with what we call the “Traub (default)” channel models of Na^+ and K^+, which are the steady-state values and time constants for m, h, and n as described by Traub and Miles (1991), and used in previous publications (Contreras et al. 1997; Destexhe and Pare 1999; Pospischil et al. 2008) (see Section 2 and Fig. 1). In the Traub (default) model the K^+ current has the properties of a delayed-rectifier. We injected a family of current ramps of different slopes to achieve a range of dVm/dt from 0.5 to 4.5 mV/ms (Fig. 3), as observed *in vivo* in primary sensory cortical neurons in response to sensory input (Wilent and Contreras 2005). We defined dVm/dt as voltage change from the time of current ramp onset to offset (spike threshold). This model failed to produce a relationship between dVm/dt and spike threshold in the soma (Fig. 3(b), gray symbols), and showed only a small relationship in the axon, between −56.58 and −56.88 mV for a change of 0.3 mV (Fig. 3(a), example spikes; 3B, black symbols). This was unexpected because it has been assumed that Na^+ inactivation during slower rising Vms should displace spike threshold towards more depolarized levels (Hodgkin and Huxley 1952; Noble and Stein 1966; Azouz and Gray 2000; Wilent and Contreras 2005).

To determine whether the absolute value of spike threshold influenced the relationship, we adjusted the positions of the steady-state curves for the Na^+ and K^+ currents by depolarizing the half-activation voltages of m_∞, h_∞, and n_∞ (and associated time constants). We changed the V_{SHIFT} variable (see Section 2) from $V_{SHIFT\,(m,h,n)} = -63$ mV to $V_{SHIFT(m,h,n)} =$

−55 mV which depolarized spike threshold by an arbitrarily large 10 mV. However, this did not result in a relationship between spike threshold and the preceding dVm/dt (Fig. 3(c)).

A possible explanation for the failure to observe a robust relationship in the default model may be due to a depolarized voltage-dependence for Na^+ inactivation, relative to activation. We shifted the half-activation for h_∞ alone in steps of −2 mV over a 20 mV range, from −41.1 to −61.1 mV ($V_{SHIFT(h)}$ =−63 mV to $V_{SHIFT(h)}$ =−83 mV) (Fig. 4(a)). A small relationship between dVm/dt and spike threshold in the axon between 0.5 and 2.0 mV/ms only became apparent after a large shift of −18 mV (Fig. 4(b) and (c) left). At the extreme shift of −20 mV, this relationship became more pronounced (Fig. 4(b)), but was accompanied by truncated spikes (Fig. 4(c), right). Finally, speeding up Na^+ inactivation alone by scaling the time constant of inactivation to 35 % of the default value (greater reductions resulted in spike failure – not shown) did not produce a relationship (Fig. 5). Thus, in the Traub (default) model, properties of Na^+ channel inactivation alone do not generate a relationship between dVm/dt and spike threshold without spike truncation.

3.3 Adjustment of the Traub (default) Na^+ inactivation voltage-dependence combined with slower kinetics produces a relationship between dVm/dt and spike threshold without spike truncation

In order to determine how well these findings regarding Na^+ inactivation generalize to other models, we inserted a different set of widely used channel models, described by Mainen et al. (1995) (referred to below as “Mainen”), into our three-compartment model (see Section 2). We then repeated the same stimulation protocol as above. Interestingly, the Mainen model produced a robust relationship between dVm/dt and spike threshold (~4 mV) without spike truncation (Fig. 6). Thus, the lack of a relationship is not a default feature of all channel models.

In order to understand how the relationship emerged using the Mainen model, we compared the steady-state activation curves and kinetics to those of the Traub (default) model (Fig. 7). Importantly, the relative positions of the steady-state Na^+ activation and inactivation curves were very different between the two models (Fig. 7(a)), resulting in very different activation/inactivation windows (Fig. 7(b)). Na^+ inactivation occurs at much more hyperpolarized values in the Mainen model compared to Traub (default), resulting in a much smaller activation/inactivation window for Na^+ to become self-sustaining and produce a spike. However, this hyperpolarized inactivation voltage does not result in spike truncation, as observed above for the Traub (default) model (see Fig. 4(c)).

Comparison of each gating variable and its kinetics between the models (Fig. 7(c)) revealed important differences in Na^+ inactivation and K^+ activation. The Mainen model Na^+ inactivation curve is very similar to the Traub (default) model in which the half-activation voltage was hyperpolarized by 20 mV ($V_{SHIFT(h)}$=−83 mV). However, the slope of the Mainen steady-state inactivation curve is different and the time constant is twice as large. Furthermore, in the Mainen model the half-activation voltage of K^+ activation is depolarized by ~30 mV and thus only serves to re-polarize the spike and not influence threshold dynamics. We hypothesized that the small differences in Na^+ inactivation slope and kinetics were capable of producing a relationship between spike threshold and dVm/dt without spike truncation.

We first adjusted the steady-state Na^+ inactivation curve of the Traub model to match that of the Mainen model. We adjusted the slope of the curve and hyperpolarized the half-activation voltage by 18 mV ($V_{SHIFT(h)}$=−81 mV) to produce what we called the Traub (adjusted) model (Fig. 8(a), *left*) (see Section 2). This change resulted in a relationship between spike threshold and dVm/dt, but still with significant spike truncation (Fig. 8(b)). The

hyperpolarization of the steady-steady inactivation curve obligatorily shifts the time-constant of inactivation without changing its magnitude. Therefore, we next increased by a factor of two the time constant for Na^+ inactivation of the Traub (adjusted) model, in order to match more closely that of Mainen (Fig. 8(a), *middle*). This change greatly reduced spike truncation and still produced a robust spike threshold relationship (Fig. 8(c)). Finally, with this model (Traub (adjusted) with $\tau_h * 2$) we depolarized the half-activation voltage of K^+ activation by 30 mV ($V_{SHIFT(n)}$=−33 mV) in order remove any influence of K^+ current (Fig. 8(a), *right*). This further reduced spike truncation while producing a spike threshold relationship (Fig. 8(d)). Thus, Na^+ inactivation can account for the relationship between spike threshold and dVm/dt when Na^+ inactivation is hyperpolarized. However to reduce spike truncation the time constant of inactivation must be appropriately large, and Na^+ must not be antagonized by an outward current.

3.4 Adjustment of the voltage-dependence of the K^+ current is sufficient to observe a relationship between dVm/dt and spike threshold in the Traub (default) model

Recently, it was shown that block of Kv1 channels abolishes the relationship between dVm/dt and spike threshold in cortical pyramidal neurons (Higgs and Spain 2011). Thus we next explored the mechanism by which K^+ currents alone can produce this relationship, and returned to the Traub (default) model in which such a relationship is absent. Kv1 channels mediate the D-current (originally described by Storm (1988)), an important feature of which is a sub-threshold activation voltage. To capture the sub-threshold activation of I_D, we shifted the activation-voltage of K^+ to more hyperpolarized values by adjusting the V_{SHIFT} parameter for n (Fig. 9(a)) (see Section 2). When adjusted in steps of 2 mV from "default" $V_{SHIFT(n)}$ =−63 mV to "shifted" $V_{SHIFT(n)}$ =−75 mV (total shift of −12 mV), a clear relationship between dVm/dt and spike threshold emerged (Fig. 9(b)). Normalizing each spike threshold to the most hyperpolarized value for each curve revealed that, for a shift of −12 mV ($V_{SHIFT(n)}$ =−75 mV), spike threshold changed by 2.5 mV in the axon and 3.0 mV in the soma over the dVm/dt range of 0.5 to 4.5 mV/ms (Fig. 9(b) bottom). The relationship is clear in a set of example spikes over the dVm/dt range (Fig. 9(c), spike threshold highlighted by the red line). We note that the threshold change is 0.5 mV larger in the soma (Fig. 9(b)). This is due to spike initiation occurring in the axon: the spike threshold reported at the soma is contaminated by the injected current. This highlights that although spike threshold measurements made at the soma most likely reflect the spike threshold in the axon, it is an indirect measure and includes some error (McCormick et al. 2007; Yu et al. 2008), even in this simple model.

Finally, we tested whether other parameters of the K^+ current alone could have a significant impact on the relationship between dVm/dt and spike threshold. Increasing the total K^+ conductance ($\bar{g}_K$) by ten times did not result in a relationship either at the axon or the soma (Fig. 10(a)). Neither did speeding up K^+ activation by scaling the time constant of activation (τ_n) to 25 % of the default value (Fig. 10(b)). Thus the voltage dependence of the outward current is important, and these simulations suggest it must activate prior to spike threshold to produce a relationship with the preceding dVm/dt.

3.5 An outward current prior to spike threshold is necessary to antagonize the Na^+ inward current and produce a relationship between dVm/dt and spike threshold

To understand the effect of shifting the activation voltage of n_∞ we made phase plots of the total trans-membrane ionic current (i.e., excluding injected current) for all spikes as a function of Vm for the default model and for $V_{SHIFT(n)}$=−75 mV (−12 mV shift) (Fig. 11). The full trajectory of the currents is very similar for both conditions indicating that the n_∞ shift does not affect the overall shape of the spikes (Fig. 11(a), top row). With default parameters, the ramps drove total ionic current that was only net inward from stimulus onset

to spike threshold and led to a tight clustering of spike thresholds (−56.58 to −56.88 mvV) over a narrow range of inward currents (−0.035 to −0.0189 mA/cm^2) (Fig. 11(a), middle and bottom left, spike thresholds indicated by black dots). When n_∞ was shifted ($V_{SHIFT(n)}$=−75 mV), a net outward current became progressively more prominent with slower ramps and antagonized the inward current prior to spike threshold (Fig. 11(a), middle and bottom right). The n_∞ shift depolarized and expanded the range of spike thresholds (−53.41 to −55.87 mV) and increased the range of inward currents at threshold (0.001 to −0.025 mA/cm^2). Examining the total ionic current at threshold (Fig. 11(a), bottom) revealed for default parameters a small but consistent trend towards larger inwards currents as the threshold slightly increased. In stark contrast, the presence of a net outward current prior to spike threshold forced the Vm to reach more depolarized levels before the inward Na^+ current became self-sustaining and reduced the net inward current at threshold (Fig. 11(a), bottom right). This depolarization of threshold lead to higher values of m over a much larger range (Fig. 11(b); $V_{SHIFT(n)}$=−75, green symbols), compared with the default model (Fig. 11(b), default). In addition, displacing n_∞ led to slightly lower values of h (and thus more Na^+ inactivation) for the longer ramps compared to the default model (Fig. 11(b), blue symbols). Thus, the overall consequence of displacing n_∞ is to force more Na^+ channels to open before their activation becomes self-sustaining to generate a spike. We next asked whether this was due to the K^+ current itself, or due to the increase in Na^+ inactivation observed (Fig. 11(b), blue symbols).

In order to test whether Na^+ inactivation produced the relationship, in the model with n_∞ shifted ($V_{SHIFT(n)}$=−75), we also shifted the half-activation voltage of h_∞ by +10 mV in the axon ($V_{SHIFT(h)}$=−53). This arbitrarily large shift was chosen in order to remove Na^+ inactivation at the voltage threshold for spike initiation. With these parameters, a relationship between dVm/dt and spike threshold was still present (although it began to break down for the two slowest rising Vms) (Fig. 12(a) and (b)). However, the observed relationship was not due to Na^+ inactivation since the value of h measured at threshold remained near 1 for all ramp durations (Fig. 12(c), blue symbols). Therefore, our simulations show that the primary mechanism underlying the increase in threshold with slower ramps is the development of an ionic outward current that prevents Na^+ activation from becoming self-sustaining. The exception is for larger values of m, for which Na^+ inactivation augments the outward current.

3.6 Increasing $\overline{g}_K$ and decreasing τ_n reduces the magnitude of the half-activation shift necessary for the K^+ current

Our previous simulations found that changing the kinetics of activation or the conductance density of the K^+ current alone were insufficient to produce a relationship (Fig. 9). However, we hypothesized that the necessary magnitude of the shift of the half-activation voltage of n_∞ could be influenced by these parameters. Indeed, a shift in the half-activation of n_∞ of only 6 mV rather than 12 mV as described above ($V_{SHIFT(n)}$=−69 mV versus $V_{SHIFT(n)}$=−75 mV) was necessary when combined with increasing $\overline{g}_K$ from 0.2 s/cm2 to 1 s/cm2 and decreasing τ_n by 75 % (Fig. 13(a)). Thus a less dramatic shift in the half-activation of the K^+ current is necessary when the channels are in higher density and activate more quickly. An increase in conductance density without changing the time constant also produced a relationship, however the most robust linear relationship required all three parameter adjustments (Fig. 13(b)). Regardless, a hyperpolarized activation voltage is the crucial feature necessary to produce a relationship between spike threshold and dVm/dt.

3.7 The effect of shifting the K^+ activation voltage is independent of model complexity and recording site

Finally, we sought to generalize our above findings regarding the effect of shifting the half-activation voltage of K^+. Recordings in the above simulations were made in the center of the axon initial segment and the soma. We repeated the simulations using Traub (default) and with $V_{SHIFT(n)}$=−75 while recording off center in both the axon and soma (25 % of the distance from both ends of each compartment). The results were unaffected by these different recording locations (data not shown). Next we repeated the above simulations in a single compartment model (Fig. 13(c)) (see Section 2). Using the Traub (default) channel models, no relationship was observed between dVm/dt and spike threshold (Fig. 13(c), middle and bottom). However, adjustment of the half-activation voltage of K^+ by 10 mV ($V_{SHIFT(n)}$=−73) produced a robust relationship (Fig. 13(c)). Thus, our results are reproducible in a single compartment model.

4 Discussion

The voltage-threshold for spike initiation is dependent on the rate of rise of the membrane potential (dVm/dt) in many types of neurons. Here we used a biophysical model to determine how properties of intrinsic membrane currents located in the axon contribute to this relationship. Na^+ inactivation was capable of producing this relationship, but required a hyperpolarized steady-state inactivation curve combined with changes in the inactivation kinetics. Furthermore, we show that an outward current activating in a sub-threshold voltage range is sufficient to antagonize the Na^+ inward current to prevent it from becoming self-sustaining at a fixed voltage threshold. Recently it was shown in cortical neurons *in vitro* that the relationship between dVm/dt and spike threshold is sensitive to block of the D-current (Higgs and Spain 2011), an axonal K^+ current that activates in a sub-threshold voltage range. Our simulations indicate the biophysical mechanism by which such a K^+ current mediates this relationship.

4.1 Adjustment of the K^+ current in the model results in an outward current with features similar to the D-current

The Traub (default) model demonstrated only a minimal relationship between dVm/dt and spike threshold (see Fig. 3). Systematic adjustment of the K^+ current activation voltage allowed for a net outward current prior to threshold (Fig. 11) and the emergence of a relationship between dVm/dt and spike threshold (Fig. 9). Activation prior to spike initiation is a key feature of the D-current and its ability to regulate spike threshold (Storm 1988). Block of the D-current with α-dendrotoxin (α-DTX) results in a loss of the relationship between dVm/dt and spike threshold in layer 2/3 pyramidal neurons of motor cortex (Higgs and Spain 2011) and auditory brainstem neurons (Ferragamo and Oertel 2002). Furthermore, adjustment of the K^+ current resulted in a linear depolarization of spike threshold, another commonly observed feature of the D-current (Bekkers and Delaney 2001; Dodson et al. 2002; Shen et al. 2004; Guan et al. 2007; Shu et al. 2007a). Although our K^+ current model lacks inactivation, the time constant for D-current inactivation is large (>2 s; (Storm 1988; Guan et al. 2006)) and thus does not play a role in regulating spike threshold for the first spike as investigated here. Finally, in our model, increasing the speed of activation and increasing the conductance density of the K^+ current allowed for a less extreme shift of the activation voltage necessary to observe the relationship (hyperpolarization of −6 mV rather than −12 mV). This is also in agreement with the fast activation kinetics of the D-current (Storm 1988; Guan et al. 2006), and the recent finding that the D-current is potentially the most prominent K^+ current in the axon initial segment of cortical neurons (Kole et al. 2007).

4.2 Limitations of the model and technical considerations

Our simulation was highly simplified, consisting of only two voltage-gated conductances in a three-compartment model. The axons of real neurons, the site of action potential initiation (Mainen et al. 1995; Stuart et al. 1997; Palmer and Stuart 2006; Shu et al. 2007b; Foust et al. 2010), are obviously vastly more complex (for two recent reviews see Bender and Trussell (2012) and Kole and Stuart (2012)). However, our goal was to systematically determine the means by which an outward current activated prior to spike threshold regulates the voltage threshold as a function of dVm/dt. Thus, we chose to start with conditions in which such a current was absent, and then to modify the existing K^+ current in order to determine which properties that current must have in order to produce the relationship. Furthermore this simplified our search for the key biophysical mechanism by which this current mediates the relationship. Finally, the morphology and physiology of the axon in our model is also highly simplified. As discussed below, the axon initial segment of real neurons is highly complex, with a gradient of Na^+ and K^+ currents of different subunit compositions. Further complicating the matter, there is debate regarding what precisely defines the axon initial segment, what the different conductance densities are along it, and the fact that there is considerable variability among different cell types (Bender and Trussell 2012; Kole and Stuart 2012). Our goal was simply to model a compartment separate from the soma in which action potentials initiate. Our interest was in the measurements of spike threshold and dVm/dt made in these two different compartments, as stimuli were delivered to the soma and action potentials back-propagated from the axon compartment to the soma compartment.

4.3 Na^+ and K^+ channels in the AIS and the regulation of action potentials

The physiology of the axon initial segment is complex, and there is variability among different neuronal subtypes (Lorincz and Nusser 2008; Bender and Trussell 2012). However, some generalizations can be made with regard to the distributions of Na^+ and K^+ channels, and how this affects action potential initiation. Kv1 channels are particularly dense in the axon initial segment (Debanne et al. 2011; Bender and Trussell 2012; Kole and Stuart 2012). This includes the D-current, which is estimated to contribute 50–75 % of the total axonal K^+ current in layer 5 pyramidal neurons (Kole et al. 2007; Shu et al. 2007a). The D-current is sensitive to α-DTX, which specifically blocks channels that include Kv1.1, Kv1.2, or Kv1.6 subunits (Harvey and Robertson 2004). In cortical pyramidal neurons, Kv1.2 was proposed to primarily mediate this current (Shu et al. 2007a). Interestingly, Kv1.2 channels are concentrated in the distal axon initial segment (Inda et al. 2006; Van Wart et al. 2007) and co-localize with Na^+ channels containing the Nav1.6 subunit (Van Wart et al. 2007; Lorincz and Nusser 2008). Recently Hu et al. (2009) showed that Nav1.6 channels specifically mediate a low voltage-threshold Na^+ current in pyramidal neurons, previously identified by Colbert and Pan (2002). The Nav1.6 channels are located in the distal axon initial segment (30–50 μm from the soma), are proposed to mediate action potential initiation, and are segregated from higher voltage-threshold Nav1.2 channels located more proximal to the soma (Hu et al. 2009). Thus K^+ channels that mediate the D-current are strategically located to regulate the initiation of action potentials, and to antagonize this low-threshold Na^+ current which is present in high densities (Kole et al. 2008).

The D-current is of course not the only K^+ current located in the axon initial segment, however evidence indicates it primarily mediates the relationship between dVm/dt and spike threshold. The A-current is very similar to the D-current, with the exception that it includes the Kv1.4 subunit and inactivates quickly, within 50 ms (Rudy 1988). However, the A-current may play a limited role in the axon initial segment of cortical pyramidal neurons. Kole et al. (2007) found that it contributed less than 10 % to the total outward current, and Colbert and Pan (2002) rarely observed the current in patching experiments. Finally, The M-current is also found in the axon initial segment and activates at sub-threshold voltages,

however it activates slowly and is composed of Kv7 channels, and is thus not affected by α-DTX (Brown and Adams 1980; Brown and Passmore 2009).

4.4 Functional roles of spike threshold regulation and the D-current

Wilent and Contreras (2005) demonstrated that the relationship between dVm/dt and spike threshold enhances the selectivity of somatosensory cortical neurons to specific sensory inputs *in vivo*. Specifically, they found that neurons of rat whisker "barrel" cortex responded to whisker deflections in a preferred direction with a more steeply rising Vm and hyperpolarized spike threshold than for deflections in the opposite direction. The lower spike threshold of the faster rising synaptic response in turn led to an increase in spike probability and an effective increase in the response to the preferred direction. Thus, spike threshold regulation was shown to play a specific computational role in cortical neurons *in vivo*. However, they did not identify the mechanism underlying this relationship, and speculated that Na^+ channel inactivation could explain their result. In context of our modeling results, and the results of Higgs and Spain (2011) in motor cortex neurons *in vitro*, we hypothesize that the relationship observed in barrel cortex neurons is mediated by a K^+ current activating in a sub-threshold voltage range, such as the D-current.

Interestingly, the expression of D-current appears to be region and neuron subtype specific. Data from Miller et al. (2008) suggest this current is found in pyramidal-tract type layer 5 neurons in primary motor cortex but not neurons of the same type in primary somatosensory cortex. Furthermore, in brainstem auditory neurons this current is found in octopus cells that require fast dVm/dt rates in order to fire, but not neighboring T stellate cells which are less sensitive to dVm/dt (Ferragamo and Oertel 2002). Thus the presence or absence of sub-threshold Kv1 axonal K^+ currents that antagonize Na^+ currents at the site of spike initiation could regulate sensitivity to synchronous inputs in a cell type specific manner.

References

Azouz R, Gray CM. Dynamic spike threshold reveals a mechanism for synaptic coincidence detection in cortical neurons *in vivo*. Proceedings of the National Academy of Sciences of the United States of America. 2000; 97:8110–8115. [PubMed: 10859358]

Azouz R, Gray CM. Adaptive coincidence detection and dynamic gain control in visual cortical neurons *in vivo*. Neuron. 2003; 37:513–523. [PubMed: 12575957]

Bekkers JM, Delaney AJ. Modulation of excitability by alpha-dendrotoxin-sensitive potassium channels in neocortical pyramidal neurons. Journal of Neuroscience. 2001; 21:6553–6560. [PubMed: 11517244]

Bender KJ, Trussell LO. The physiology of the axon initial segment. Annual Review of Neuroscience. 2012; 35:249–265.

Brown DA, Adams PR. Muscarinic suppression of a novel voltage-sensitive K+ current in a vertebrate neurone. Nature. 1980; 283:673–676. [PubMed: 6965523]

Brown DA, Passmore GM. Neural KCNQ (Kv7) channels. British Journal of Pharmacology. 2009; 156:1185–1195. [PubMed: 19298256]

Bryant HL, Segundo JP. Spike initiation by transmembrane current: a white-noise analysis. Journal of Physiology. 1976; 260:279–314. [PubMed: 978519]

Cardin JA, Kumbhani RD, Contreras D, Palmer LA. Cellular mechanisms of temporal sensitivity in visual cortex neurons. Journal of Neuroscience. 2010; 30:3652–3662. [PubMed: 20219999]

Colbert CM, Pan E. Ion channel properties underlying axonal action potential initiation in pyramidal neurons. Nature Neuroscience. 2002; 5:533–538.

Contreras D, Destexhe A, Steriade M. Intracellular and computational characterization of the intracortical inhibitory control of synchronized thalamic inputs *in vivo*. Journal of Neurophysiology. 1997; 78:335–350. [PubMed: 9242284]

Debanne D, Campanac E, Bialowas A, Carlier E, Alcaraz G. Axon physiology. Physiological Reviews. 2011; 91:555–602. [PubMed: 21527732]

Destexhe A, Pare D. Impact of network activity on the integrative properties of neocortical pyramidal neurons *in vivo*. Journal of Neurophysiology. 1999; 81:1531–1547. [PubMed: 10200189]

Destexhe, A.; Sejnowski, TJ. Thalamocortical assemblies: How ion channels, single neurons, and large-scale networks organize sleep oscillations. Oxford University Press; New York: 2001.

Destexhe A, Rudolph M, Fellous JM, Sejnowski TJ. Fluctuating synaptic conductances recreate *in vivo*-like activity in neocortical neurons. Neuroscience. 2001; 107:13–24. [PubMed: 11744242]

Dodson PD, Barker MC, Forsythe ID. Two heteromeric Kv1 potassium channels differentially regulate action potential firing. Journal of Neuroscience. 2002; 22:6953–6961. [PubMed: 12177193]

Ferragamo MJ, Oertel D. Octopus cells of the mammalian ventral cochlear nucleus sense the rate of depolarization. Journal of Neurophysiology. 2002; 87:2262–2270. [PubMed: 11976365]

Foust A, Popovic M, Zecevic D, McCormick DA. Action potentials initiate in the axon initial segment and propagate through axon collaterals reliably in cerebellar Purkinje neurons. Journal of Neuroscience. 2010; 30:6891–6902. [PubMed: 20484631]

Goldberg EM, Clark BD, Zagha E, Nahmani M, Erisir A, Rudy B. K+ channels at the axon initial segment dampen near-threshold excitability of neocortical fast-spiking GABAergic interneurons. Neuron. 2008; 58:387–400. [PubMed: 18466749]

Guan D, Lee JC, Tkatch T, Surmeier DJ, Armstrong WE, Foehring RC. Expression and biophysical properties of Kv1 channels in supragranular neocortical pyramidal neurones. The Journal of Physiology. 2006; 571:371–389. [PubMed: 16373387]

Guan D, Lee JC, Higgs MH, Spain WJ, Foehring RC. Functional roles of Kv1 channels in neocortical pyramidal neurons. Journal of Neurophysiology. 2007; 97:1931–1940. [PubMed: 17215507]

Harvey AL, Robertson B. Dendrotoxins: structure-activity relationships and effects on potassium ion channels. Current Medicinal Chemistry. 2004; 11:3065–3072. [PubMed: 15579000]

Henze DA, Buzsaki G. Action potential threshold of hippocampal pyramidal cells *in vivo* is increased by recent spiking activity. Neuroscience. 2001; 105:121–130. [PubMed: 11483306]

Higgs MH, Spain WJ. Kv1 channels control spike threshold dynamics and spike timing in cortical pyramidal neurones. Journal of Physiology. 2011; 589:5125–5142. [PubMed: 21911608]

Hines ML, Carnevale NT. The NEURON simulation environment. Neural Computation. 1997; 9:1179–1209. [PubMed: 9248061]

Hodgkin AL, Huxley AF. A quantitative description of membrane current and its application to conduction and excitation in nerve. The Journal of Physiology. 1952; 117:500–544. [PubMed: 12991237]

Hu W, Tian C, Li T, Yang M, Hou H, Shu Y. Distinct contributions of Na(v)1.6 and Na(v)1.2 in action potential initiation and backpropagation. Nature Neuroscience. 2009; 12:996–1002.

Inda MC, DeFelipe J, Munoz A. Voltage-gated ion channels in the axon initial segment of human cortical pyramidal cells and their relationship with chandelier cells. Proceedings of the National Academy of Sciences of the United States of America. 2006; 103:2920–2925. [PubMed: 16473933]

Kole MH, Stuart GJ. Signal processing in the axon initial segment. Neuron. 2012; 73:235–247. [PubMed: 22284179]

Kole MH, Letzkus JJ, Stuart GJ. Axon initial segment Kv1 channels control axonal action potential waveform and synaptic efficacy. Neuron. 2007; 55:633–647. [PubMed: 17698015]

Kole MH, Ilschner SU, Kampa BM, Williams SR, Ruben PC, Stuart GJ. Action potential generation requires a high sodium channel density in the axon initial segment. Nature Neuroscience. 2008; 11:178–186.

Lorincz A, Nusser Z. Cell-type-dependent molecular composition of the axon initial segment. Journal of Neuroscience. 2008; 28:14329–14340. [PubMed: 19118165]

Mainen ZF, Joerges J, Huguenard JR, Sejnowski TJ. A model of spike initiation in neocortical pyramidal neurons. Neuron. 1995; 15:1427–1439. [PubMed: 8845165]

McCormick DA, Shu Y, Yu Y. Neurophysiology: Hodgkin and Huxley model—still standing? Nature. 2007; 445:E1–E2. discussion E2-3. [PubMed: 17203021]

Miller MN, Okaty BW, Nelson SB. Region-specific spike-frequency acceleration in layer 5 pyramidal neurons mediated by Kv1 subunits. Journal of Neuroscience. 2008; 28:13716–13726. [PubMed: 19091962]

Noble D. Applications of Hodgkin-Huxley equations to excitable tissues. Physiological Reviews. 1966; 46:1–50. [PubMed: 5323501]

Noble D, Stein RB. The threshold conditions for initiation of action potentials by excitable cells. The Journal of Physiology. 1966; 187:129–162. [PubMed: 16992236]

Palmer LM, Stuart GJ. Site of action potential initiation in layer 5 pyramidal neurons. Journal of Neuroscience. 2006; 26:1854–1863. [PubMed: 16467534]

Pospischil M, Toledo-Rodriguez M, Monier C, Piwkowska Z, Bal T, Fregnac Y, et al. Minimal Hodgkin-Huxley type models for different classes of cortical and thalamic neurons. Biological Cybernetics. 2008; 99:427–441. [PubMed: 19011929]

Rudy B. Diversity and ubiquity of K channels. Neuroscience. 1988; 25:729–749. [PubMed: 2457185]

Schlue WR, Richter DW, Mauritz KH, Nacimiento AC. Responses of cat spinal motoneuron somata and axons to linearly rising currents. Journal of Neurophysiology. 1974; 37:303–309. [PubMed: 4815207]

Shen W, Hernandez-Lopez S, Tkatch T, Held JE, Surmeier DJ. Kv1.2-containing K+ channels regulate subthreshold excitability of striatal medium spiny neurons. Journal of Neurophysiology. 2004; 91:1337–1349. [PubMed: 13679409]

Shu Y, Yu Y, Yang J, McCormick DA. Selective control of cortical axonal spikes by a slowly inactivating K+ current. Proceedings of the National Academy of Sciences of the United States of America. 2007a; 104:11453–11458. [PubMed: 17581873]

Shu Y, Duque A, Yu Y, Haider B, McCormick DA. Properties of action-potential initiation in neocortical pyramidal cells: evidence from whole cell axon recordings. Journal of Neurophysiology. 2007b; 97:746–760. [PubMed: 17093120]

Storm JF. Temporal integration by a slowly inactivating K+ current in hippocampal neurons. Nature. 1988; 336:379–381. [PubMed: 3194020]

Stuart G, Schiller J, Sakmann B. Action potential initiation and propagation in rat neocortical pyramidal neurons. The Journal of Physiology. 1997; 505(Pt 3):617–632. [PubMed: 9457640]

Traub, RD.; Miles, R. Neuronal networks of the hippocampus. Cambridge University Press; Cambridge: 1991.

Van Wart A, Trimmer JS, Matthews G. Polarized distribution of ion channels within microdomains of the axon initial segment. The Journal of Comparative Neurology. 2007; 500:339–352. [PubMed: 17111377]

Wilent WB, Contreras D. Stimulus-dependent changes in spike threshold enhance feature selectivity in rat barrel cortex neurons. Journal of Neuroscience. 2005; 25:2983–2991. [PubMed: 15772358]

Yu Y, Shu Y, McCormick DA. Cortical action potential backpropagation explains spike threshold variability and rapidonset kinetics. Journal of Neuroscience. 2008; 28:7260–7272. [PubMed: 18632930]

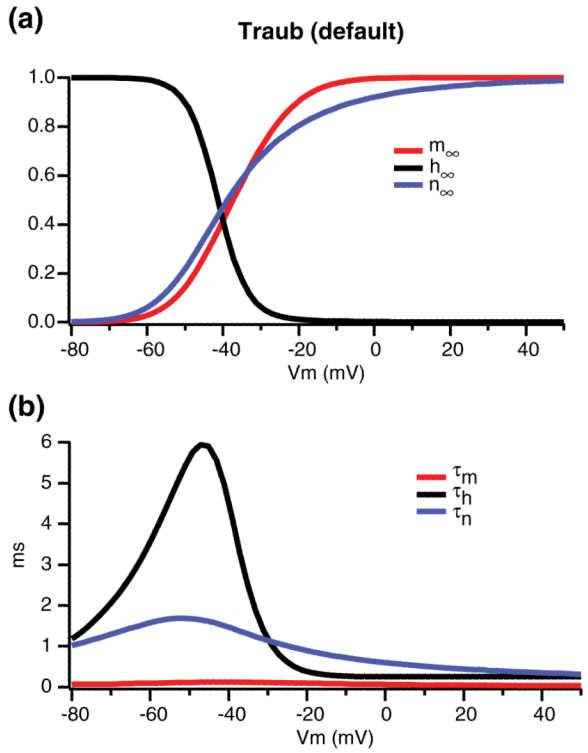

Fig. 1.

Traub (default) model of the Na^+ and K^+ currents used in this study. (**a**) Steady-state activation values for the Traub (default) model (rate constants defined in the Section 2; $V_{SHIFT(m,h,n)}$=−63). (**b**) Time constants for activation

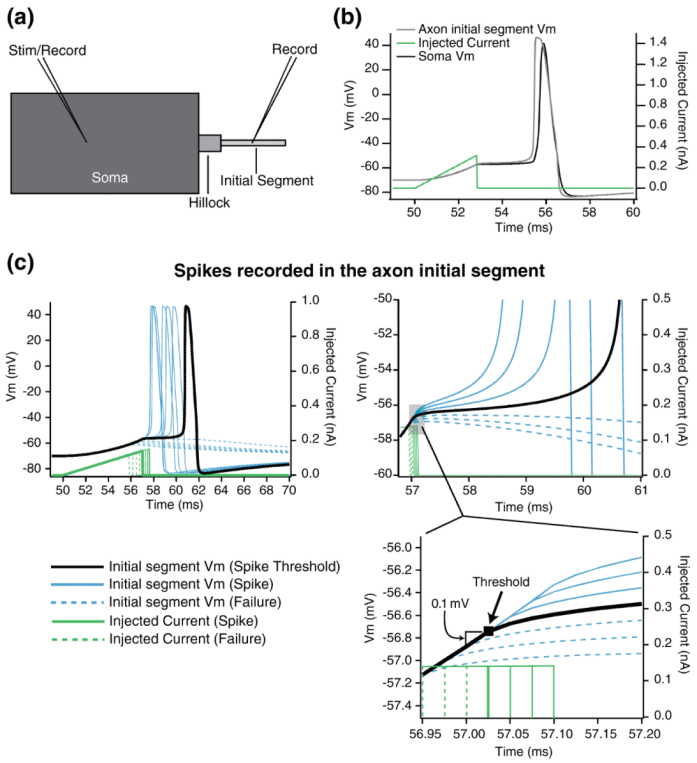

Fig. 2.

Simulation design. (**a**) Three-compartment model with soma, axon hillock, and axon initial segment. Stimulation current was applied to the soma compartment and recordings were made in the soma and axon initial segment. (**b**) Ramps of current injected at the soma controlled the dVm/dt prior to a spike. Spikes were initiated in the axon initial segment and back-propagated to the soma. (**c**) The voltage threshold for spiking was determined empirically. All spikes shown are from the axon compartment. *Left.* Examples of spikes caused by supra-threshold stimulation (*solid blue*), spike failures caused by sub-threshold stimulation (*dashed blue*), and a spike caused by depolarization within 0.1 mV of threshold (*solid black*). *Right.* Close-up of spikes and spike failures. The *bottom right* shows that spike threshold (indicated by *black square*) was determined within 0.1 mV of sub-threshold (noted by *bracket* and *arrow*) and supra-threshold Vm values. Note that at the time of current ramp off-set, all Vm trajectories are determined by intrinsic membrane currents

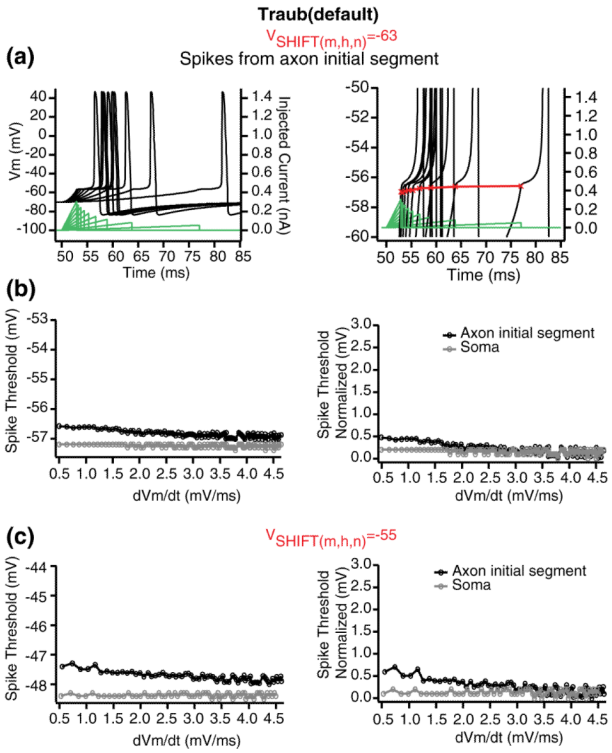

Fig. 3.

The Traub (default) model fails to produce a relationship between dVm/dt and spike threshold. (**a**) A set of example spikes from the axon with dVm/dt values between 0.5 and 4.5 mV/ms for the Traub (default) model ($V_{SHIFT(m,h,n)}$=−63). At *right* is a closeup near spike threshold, showing that threshold values do not change along with dVm/dt. Red crosses (and *line*) indicate the spike thresholds. (**b**) Spike threshold as a function of dVm/dt in the axon (*black*) and soma (*gray*). At *right*, spike thresholds were normalized to the most hyperpolarized value in order to show the net change. A change of ~0.3 mV occurs only in the axon compartment over the range of dVm/dt values. (**c**) The half-activation for all variables were shifted to more depolarized values ($V_{SHIFT(m,h,n)}$=−55 for *m*, *h*, and *n*). This depolarized the spike threshold, but did not result in a relationship with dVm/dt

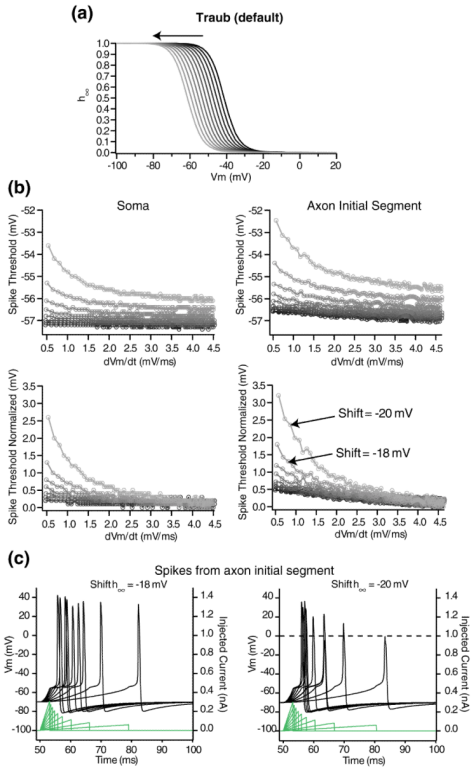

Fig. 4.

Adjustment of the activation voltage for Na^+ inactivation in the Traub (default) model only results in a relationship at extreme values. (**a**) The half-activation voltage of h_∞ was hyperpolarized by 20 mV in steps of −2 mV ($V_{SHIFT(h)}$=−63 to −83). (**b**) Spike threshold as a function of dVm/dt in the soma (*left*) and axon (*right*). The colors correspond to the adjustment of h_∞ in part A. *Bottom*. Spike thresholds were normalized to the most hyperpolarized in order to show the net change. A robust relationship only begins to emerge for the two most extreme adjustments of −18 ($V_{SHIFT(h)}$=−81) and −20 mV ($V_{SHIFT(h)}$= −83), but over a limited range of dVm/dt values. (**c**) A set of example spikes with dVm/dt values between 0.5 and 4.5 mV/ms for shifts of −18 ($V_{SHIFT(h)}$=−81) (*left*) and −20 mV ($V_{SHIFT(h)}$=−83) (*right*). With a shift of −20 mV the spikes begin to truncate for slower dVm/dt values

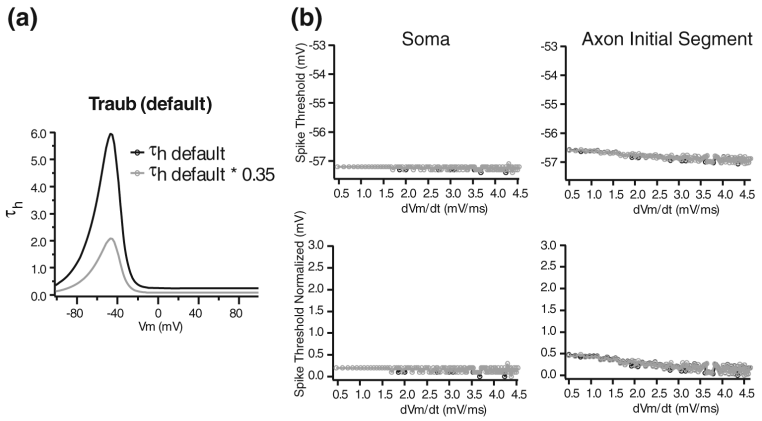

Fig. 5.

Scaling the time constant for Na^+ inactivation in the Traub (default) model does not produce a relationship between dVm/dt and spike threshold. (**a**) Time constant for Na^+ inactivation before and after scaling by 65 % (maximum before spikes truncate). (**b**) Spike threshold as a function of dVm/dt before (*black*) and after (*gray*) scaling

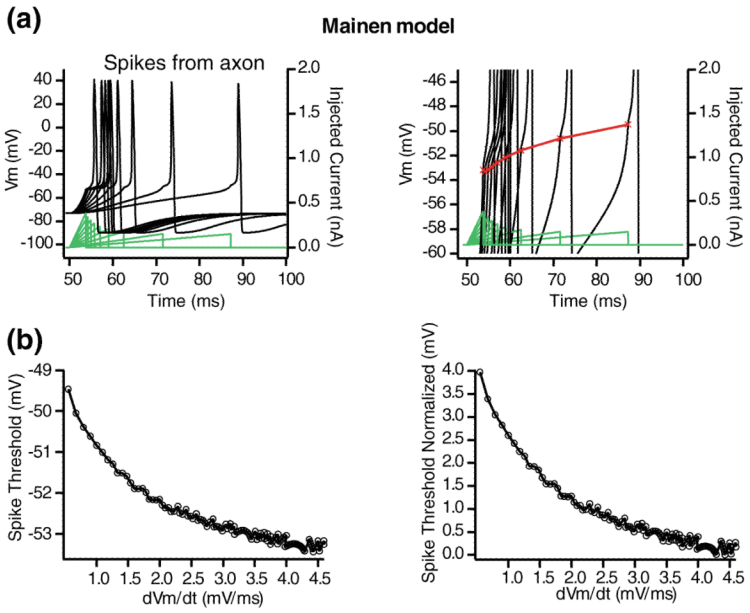

Fig. 6.

The Mainen channel models produce a relationship between dVm/dt and spike threshold. (**a**) A set of example spikes with dVm/dt values between 0.5 and 4.5 mV/ms for the Mainen model of Na^+ and K^+ channels. The expanded traces on the right demonstrate a clear relationship between dVm/dt and spike threshold. *Red line* and *crosses* indicate spike thresholds. (**b**) Spike threshold as a function of dVm/dt in the axon. At *right*, spike thresholds were normalized to the most hyperpolarized value in order to show the net change. A change of 4 mV occurs in the axon compartment over the range of dVm/dt values

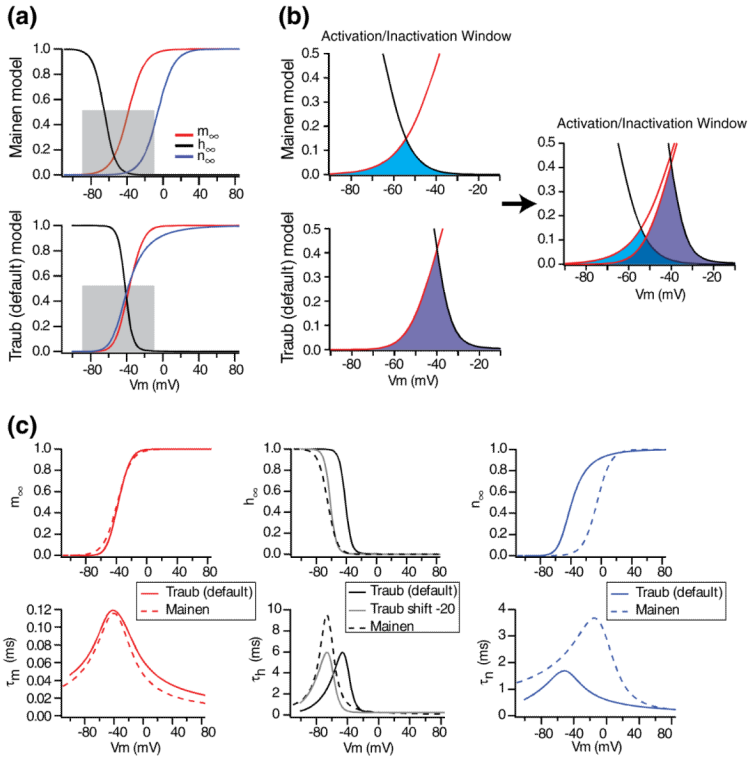

Fig. 7.

Comparison of activation curves and kinetics for the Traub (default) and Mainen models. (**a**) Steady-state activation values for the Mainen and Traub (default) models. *Gray boxes* define regions expanded in *B*. (**b**) Activation/inactivation windows for the Mainen and Traub (default) models. The activation/inactivation window for the Mainen model is smaller than Traub (default) and begins at more hyperpolarized membrane potentials. (**c**) Comparison of individual steady-state curves and kinetics. The Na^+ activation variable m is similar in voltage-dependence and kinetics between the two models. The half-activation voltage of the Mainen Na^+ inactivation variable h is similar to that of the Traub (default) model shifted by −20 mV. Also, note that the time constant for m is twice as large for the Mainen model. Finally the K^+ activation variable n is depolarized by ~30 mV in the Mainen model and thus does not contribute to spike threshold dynamics

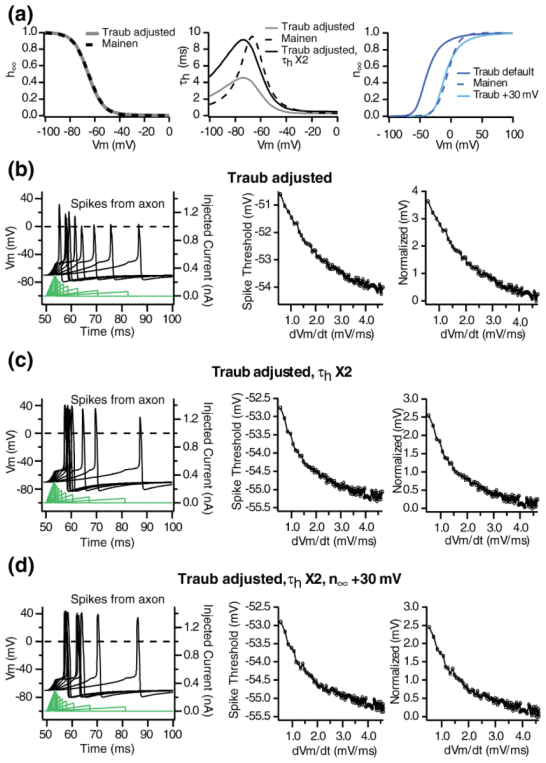

Fig. 8.

Adjustment of the Traub Na^+ inactivation and K^+ activation variables to match those of the Mainen model produces a relationship between dVm/dt and spike threshold without significant spike truncation. (**a**) Adjustments to the Traub Na^+ inactivation variable *h* and K^+ activation variable *n* used to produce the simulation results of *B–D*. The slope and activation voltage of h_∞ was adjusted to match that of Mainen in the Traub (adjusted) model (see Section 2). (**b**) Adjustment of h_∞ alone (Traub (adjusted), see *A, left*) produces a relationship between dVm/dt and spike threshold but with spike truncation. (**c**) Scaling time constant of the Traub (adjusted) variable *h* by a factor of 2 (see *A, left* and *middle*) produces a relationship between dVm/dt and spike threshold with reduced spike truncation. (**d**) Depolarization of n_∞ by 30 mV (see *A, right*) to remove K^+ during spike initiation further reduces spike truncation. This manipulation was combined that described in *C* above

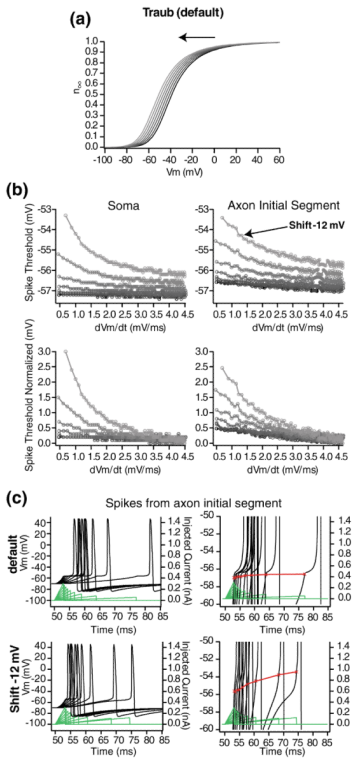

Fig. 9.

Adjustment of the Traub (default) activation voltage for K^+ results in a relationship between dVm/dt and spike threshold. (**a**) The Traub (default) model half-activation voltage of n_∞ was hyperpolarized by 12 mV in steps of 2 mV ($V_{SHIFT(n)}$=−63 to −75) in the axon. (**b**) Spike threshold as a function of dVm/dt in the soma (*left*) and axon (*right*). The colors correspond to the adjustment of n_∞ in part *B*. *Bottom*. Spike thresholds were normalized to the most hyperpolarized in order to show the net change. A relationship begins to emerge as the activation voltage is hyperpolarized. The relationship obtained from the shift used in part *C* below is noted by the arrow (Shift −12 mV). (**c**) A set of example spikes with dVm/dt values between 0.5 and 4.5 mV/ms for the default model (*top*: $V_{SHIFT(n)}$=−63) and with the half-activation for the K^+ current hyperpolarized in the axon (*bottom*: $V_{SHIFT(n)}$=−75). *Red line* and *crosses* indicate the spike thresholds; note depolarization of spike threshold as dVm/dt becomes slower on the *bottom row*

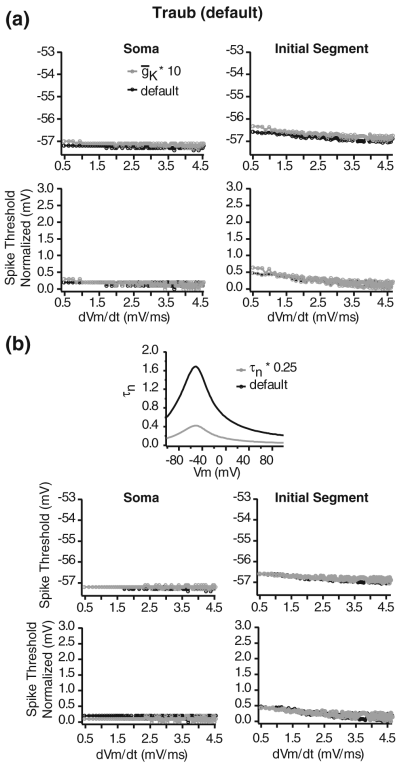

Fig. 10.

Scaling the density of the K^+ conductance or the time constant for K^+ activation alone for the Traub (default) model do not result in a relationship between dVm/dt and spike threshold. (**a**) The maximum conductance ($\bar{g}_K$) was scaled by a factor of 10 in the axon but had no effect on the relationship between dVm/dt and spike threshold. (**b**) The time constant for K^+ activation was scaled by 75 % in the axon but also had no effect

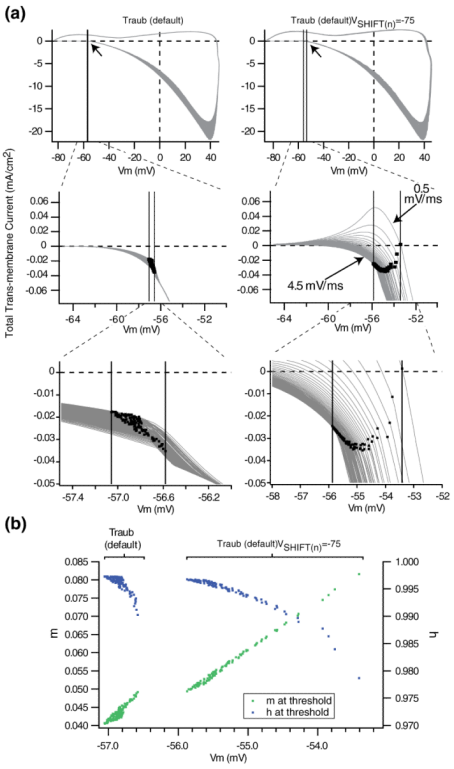

Fig. 11.

Adjustment of the activation voltage of the K^+ current in the axon generates an outward current prior to spike threshold that antagonizes the Na^+ inward current to keep it from becoming self-sustaining at a fixed voltage threshold. (**a**) *Top*. Axon initial segment total transmembrane ionic current was plotted as a function of Vm for all spikes for the Traub (default) model (*left*) and with hyperpolarization of the K^+ current ($V_{SHIFT(n)}$=−75) (*right*). *Vertical lines* bracket the range of spike thresholds over the dVm/dt range. *Arrows* denote the region of the phase plots where spike threshold occurs, which is further expanded below. *Middle*. Expansion of the region of the plots near spike threshold. *Black dots* denote the total trans-membrane ionic current at voltage threshold. Note the net inward current for all spikes in the default model (*left*). With adjustment of the K^+ current, an outward current is present prior to spike threshold and increases as dVm/dt slows (*right*). *Bottom*. Further expansion (note x-axis range is now different for default versus K^+ current shifted). In the default model there is a trend for the ionic inward current to increase as threshold depolarizes. In contrast, with the adjusted K^+ current, the net inward current at threshold is smaller for slower Vms and more depolarized thresholds. This is due to the increase in available Na^+ channels (increased *m*) as described in part *B*. (**b**) Instantaneous values of *m* and *h* in the axon at spike threshold (*green* and *blue dots*) for the default model and for adjusted K^+ current ($V_{SHIFT(n)}$=−75). This reveals that in the default model there is a narrow range of *m* values and little inactivation of Na^+ (*h* remains near 1). With adjustment of the K^+ current, the range of *m* values is expanded and all are larger (Na^+ channel availability must be larger to generate a spike) and *h* decreases (thus Na^+ channel inactivation increases) for slower rising Vm trajectories

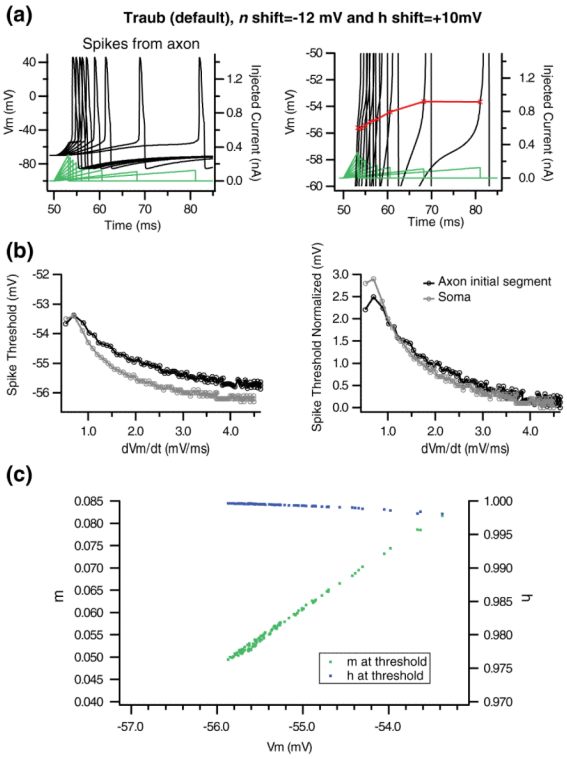

Fig. 12.

Adjustment of the activation voltage of the axonal K^+ current and removal of Na^+ inactivation at spike threshold still generates a relationship between dVm/dt. (**a**) A set of example spikes with dVm/dt values between 0.5 and 4.5 mV/ ms for K^+ activation hyperpolarized ($V_{SHIFT(n)}$=−75) and Na^+ inactivation depolarized by 10 mV ($V_{SHIFT(h)}$= −53). At right is a close-up near spike threshold, showing that threshold values change along with dVm/dt values. *Red line* and *crosses* indicate the spike thresholds. (**b**) Spike threshold as a function of dVm/dt in the axon (*black*) and soma (*gray*). The relationship between dVm/dt and spike threshold is preserved for all but the most slowly rising Vms prior to spiking. (**c**) Instantaneous values of *m* and *h* in the axon at spike threshold (*green* and *blue dots*) for the model with adjusted K^+ current ($V_{SHIFT(n)}$=−75) and Na^+ inactivation ($V_{SHIFT(h)}$=−53). The values and range of instantaneous *m* is very similar to that observed with Na^+ inactivation unadjusted (Fig. 8(c)), but *h* is near 1 for all spikes. This reveals that inactivation of Na^+ is not required to produce a relationship between dVm/dt and spike threshold; only the antagonizing outward K^+ current is necessary

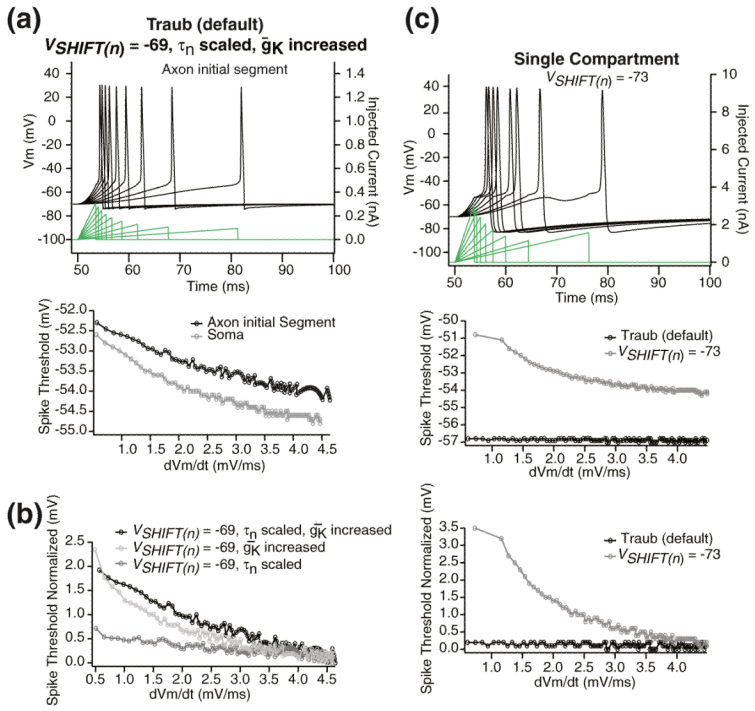

Fig. 13.

Increasing $\bar{g}_K$ and decreasing τ_n reduces the necessary magnitude of the half-activation shift for the K^+ current, and results generalize to a single compartment model. (**a**) *Top*. A set of example spikes with dVm/dt values between 0.5 and 4.5 mV/ms for K^+ activation hyperpolarized ($V_{SHIFT(n)}$=−69), $\bar{g}_K$ increased by 10, and τ_n reduced by 75 %. *Bottom*. Spike threshold as a function of dVm/dt in the axon initial segment and soma compartments quantifying the relationship. (**b**) Increasing the K^+ conductance density and decreasing the time constant for activation produces the most robust linear relationship when combined with a hyperpolarizing shift of the K^+ activation curve. However, the increase in conductance density provides a more important contribution than reducing the time constant. (**c**) Adjustment of the K^+ activation voltage produces a relationship in a single compartment model. *Top.* Example spikes from a single compartment using Traub (default) with the K^+ activation voltage hyperpolarized by 10 mV ($V_{SHIFT(n)}$=−73). *Middle and Bottom*. Spike threshold relationship as a function of dVm/dt without and without the adjustment